Natural Hazards Research 4 (2024) 97–109

Contents lists available at ScienceDirect

Natural Hazards Research

journal homepage: www.keaipublishing.com/en/journals/natural-hazards-research

Evaluating multi-hazard risk associated with tropical cyclones using the fuzzy analytic hierarchy process model

Sajib Sarker [a,c], Mohammed Sarfaraz Gani Adnan [a,b,*]

[a] Department of Urban and Regional Planning, Chittagong University of Engineering and Technology (CUET), Chattogram, 4349, Bangladesh
[b] Department of Civil & Environmental Engineering, University of Strathclyde, 75 Montrose Street, Glasgow, G1 1XJ, United Kingdom
[c] Institute of Water and Flood Management (IWFM), Bangladesh University of Engineering and Technology (BUET), Dhaka, 1000, Bangladesh

ARTICLE INFO

Keywords:
Multi-hazard
Tropical cyclone
Fuzzy analytic hierarchy process
Risk analysis
Bangladesh

ABSTRACT

Multi-hazard events have received attention globally due to their increasing frequency and severity in recent years. The coastal region of Bangladesh is particularly vulnerable to multi-hazard events induced by tropical cyclones (TC), including coastal flooding, extreme precipitation, extreme winds, and salinity intrusion. These events inflict substantial damage on human lives and property, yet there has been limited effort to quantitatively assess the associated risks. This study aims to investigate the spatial distribution of multi-hazard risks stemming from TC events, employing a Fuzzy Analytic Hierarchy Process (FAHP) approach. Risk is assessed in relation to hazard, exposure, vulnerability, and mitigation capacities in the study area. Various indicators are selected to define each of these four risk components, with weights determined through expert input for FAHP modeling. The results indicate that more than 50% of the area faces multi-hazard risks, with the hazard component exhibiting the highest degree of risk association, followed by exposure, vulnerability, and adaptive capacity. Storm surge-induced flooding is identified as the most prominent hazard during TC events, followed by intense precipitation, extreme winds, and salinity intrusion. Areas characterized by high population density, a large number of vulnerable populations (e.g., those under 15 years or over 65 years), low elevation, and underdevelopment are found to be the most risk prone. Notably, the presence of hospitals, cyclone centers, and effective warning systems in proximity to an area enhances its potential to withstand multi-hazard impacts. Among the 19 coastal districts, Cox's Bazar and Feni are identified as the most risk prone. The framework and findings presented in this study offer valuable insights for the development and prioritization of multi-hazard risk mitigation policies by identifying the most vulnerable zones and the associated risk factors.

1. Introduction

Multi-hazard risk assessment has increasingly become a crucial topic worldwide, primarily driven by the growing frequency, complexity, and interconnectedness of hazards (Gill et al., 2022). However, assessing the risks posed by multiple hazards presents significant challenges, mainly due to the intricate interactions among individual hazards, leading to compound or cascading events (Gill and Malamud, 2014; Pouyakian et al., 2022; Tilloy et al., 2019). For instance, earthquakes, storms, and floods often culminate in multi-hazard events (Akay, 2021). The cumulative impact of these multi-hazard events on both people and assets far exceeds that which would result from their individual occurrences (de Brito and Evers, 2016). Communities' vulnerability to multi-hazard situations is steadily on the rise in the context of climate change, emphasizing the need for a suitable framework to assess these risks. Such assessments are vital for informing disaster risk reduction policies and enhancing community resilience (Anwar et al., 2020).

On a global stage, multi-hazard risk assessment plays a crucial role as an indispensable tool for enhancing resilience and preparedness in an increasingly complex and interconnected world (Argyroudis et al., 2020; Bernal et al., 2017). The significance of understanding and mitigating multi-hazard risks lies in the capacity to anticipate, adapt, and respond to a spectrum of threats, ranging from natural disasters to human-induced crises (Kappes et al., 2012). Societies can develop robust strategies for disaster risk reduction by comprehensively evaluating the interactions between various hazards. This holistic approach is vital for safeguarding communities, infrastructure, and ecosystems, fostering sustainable development, and ensuring the well-being of populations worldwide

* Corresponding author. Department of Civil & Environmental Engineering, University of Strathclyde, 75 Montrose Street, Glasgow, G1 1XJ, United Kingdom.
E-mail address: mohammed.adnan@strath.ac.uk (M.S.G. Adnan).

https://doi.org/10.1016/j.nhres.2023.11.007
Received 19 October 2023; Received in revised form 10 November 2023; Accepted 13 November 2023
Available online 21 November 2023

(Argyroudis et al., 2020; Bernal et al., 2017).

Bangladesh, situate in South Asia, is vulnerable to a range of hazards, including various types of floods, cyclones, landslides, and heatwaves. This vulnerability is attributed to the country's geographical location, climatic conditions, rapid population growth, and urbanization (Shaw et al., 2013). Notably, Bangladesh is particularly susceptible to diverse flood types (Adnan et al., 2019b), cyclones (Dasgupta et al., 2014), storm surges (Murty and Flather, 1994), landslides (Sarwar, 2008), and heatwaves (Raja et al., 2021). While each of these hazards inflicts substantial damage on infrastructure, disrupts economic activities, and results in loss of life, their combined impact magnifies the losses (Barbour et al., 2022; Hoque et al., 2016).

In the coastal region of Bangladesh, tropical cyclones, in particular, pose the primary multi-hazard risk. These cyclones originate over the Bay of Bengal when warm, humid air from the Indian Ocean collides with cooler, drier air from the north. As warm air rises and cools, it creates cyclonic circulation and clouds, releasing latent heat in the process (Girishkumar and Ravichandran, 2012). These events can trigger and/or amplify secondary hazards such as storm surges, intense precipitation, salinity intrusion, high-speed winds, flooding, and landslides. The pre-monsoon and post-monsoon seasons, occurring from March to May and October to November, respectively, often coincide with tropical storm activity in Bangladesh. These seasons are characterized by high atmospheric instability and oceanic warmth, conditions conducive to the formation and intensification of tropical cyclones over the Bay of Bengal (Tiwari et al., 2022). Climate change could increase frequency and intensity of cyclones in Bangladesh in future, further elevating the nation's multi-hazard risk (Alam and Collins, 2010). To develop an effective cyclone risk management strategy, it is imperative to comprehensively understand the interdependencies and interactions between hazards, as well as the social, economic, and environmental factors associated with risk.

Most existing studies in the field of natural hazard management have primarily focused on analyzing the impacts of individual hazards (Bakkensen and Mendelsohn, 2019; Choi et al., 2021; Ward et al., 2020), a pattern observed in the context of Bangladesh as well. However, numerous studies have underscored the importance of comprehending both the geographical and temporal correlations between various hazards. They emphasize the need to consider how these diverse hazards can collectively impact social and economic systems (Bourdeau-Brien and Kryzanowski, 2020; Cutter and Finch, 2008; Wachinger et al., 2013). These studies have recognized the significance of investigating interactions and the networks of interactions (often referred to as cascades) within the realm of multiple hazards (Gill and Malamud, 2017; Tilloy et al., 2019). Given Bangladesh's susceptibility to multi-hazard events, recent research has underscored the necessity for a comprehensive approach to natural hazard management. For example, Juarez Garcia (2010) explained that traditional methods of risk assessment in Bangladesh have primarily focused on isolated hazard occurrences such as floods or cyclones, neglecting the intricate interactions among different hazards. Bianchi and Malki-Epshtein (2021) have stressed the importance of integrated, adaptable solutions that can address the nation's unique and evolving hazard landscape. They highlight the significance of adopting a multi-hazard approach to natural hazard management.

The absence of accurate data on the likelihood and severity of multiple hazards occurring simultaneously or shortly after one another is one of the main obstacles in multi-hazard risk assessment (Gill and Malamud, 2016). The severity of impacts caused by the interaction of multiple hazards is often underestimated, leading to an incomplete understanding of the risks associated with multi-hazard events. Another challenge in quantifying multi-hazard risk is the difficulty in determining the spatial and temporal dependencies between hazards (Ming et al., 2022). Hazard events can be interdependent in space and time, and the occurrence of one hazard can trigger another. In addition to the spatial and temporal dependencies between hazards, there is also the challenge of understanding the interactions between different types of hazards (Gill and Malamud, 2016). Finally, a dearth of standardized approaches to multi-hazard risk assessment is also a significant challenge. The integration of different types of hazards and the various interdependencies and interactions between them require a multidisciplinary approach that involves experts from different fields (Liu et al., 2016). Despite the difficulties, multi-hazard risk assessment is crucial for creating effective plans for reducing the likelihood of disasters and enhancing resilience to their effects.

Numerous methods for multi-hazard risk assessment exist within the literature. Nonetheless, comprehensive approaches are those that account for interdependencies and interactions between hazards while addressing the uncertainties and limitations associated with hazard modeling and data availability (Talchabhadel et al., 2023). Among these assessment methods, the Fuzzy Analytical Hierarchy Process (FAHP) method has received attention recently (Siam et al., 2022). This decision-making approach is potent and versatile, finding applications in various fields, including economics, engineering, ecological management, and urban planning. FAHP extends AHP by incorporating fuzzy sets, allowing for the representation of ambiguous or uncertain information and facilitating a more accurate simulation of human judgment and perception (Kubler et al., 2016). Alternative approaches to FAHP include integrated risk assessment (Greiving, 2006), Bayesian networks (Pearl, 2011), multi-criteria decision analysis (Montibeller and Franco, 2010), multi-hazard early warning systems (Aguirre-Ayerbe et al., 2020), and system dynamics (Naghadehi et al., 2011). While these options each possess their own strengths and weaknesses, the choice of approach should align with the specific requirements of the assessment (Ming et al., 2022).

The investigation of multi-hazard risk is fraught with challenges. Firstly, accurately modeling the interdependencies and interactions between hazards proves to be a complex endeavor (Kappes et al., 2012). Secondly, the scarcity of high-quality data, especially in low-income countries, poses a significant hurdle (Eshrati et al., 2015). Thirdly, existing methods may not fully account for the intricate social, economic, and environmental factors influencing risk, nor adequately integrate the perspectives and needs of local communities and stakeholders (Bera and Maiti, 2021). In the context of complex and dynamic cyclone-induced multi-hazard events, all these challenges are magnified (Tilloy et al., 2019). Cyclones can be influenced by a range of social and economic factors such as population density, infrastructure quality, and resource access, which may be challenging to capture using existing methods. Lastly, the impacts of cyclones can be exacerbated by climate change, heightening the frequency and intensity of cyclones and rendering existing risk management strategies ineffective (Kappes et al., 2012). To address the various challenges of multi-hazard risk assessment, this study aims to investigate cyclone-induced multi-hazard risk in the coastal region of Bangladesh.

2. Materials and methods

This study employed the Fuzzy Analytical Hierarchy Process (FAHP) approach to assess the multi-hazard risk induced by cyclones in coastal Bangladesh. Risk was defined as a function comprising hazard, exposure, vulnerability, and adaptive capacity (Hoque et al., 2019). To establish each of these four risk components, a set of indicators was selected, which are detailed in Table 1, along with their respective data sources. Fig. 1 provides an overview of the general methodological framework employed in this study.

2.1. Study area

This study was centered on the coastal region of Bangladesh (see Fig. 2), encompassing 19 out of 64 districts and home to approximately 35 million residents (Islam et al., 2017). The Bangladesh coastline, stretching over 700 kilometers, can be broadly categorized into three

Table 1
Description of various indicators related to different risk components such as hazard, exposure, capacity and vulnerability, including their data sources.

Risk components	Indicators	Description	Format	Data Source
Multi- hazard events	Storm surge induced flood inundation	The extent of storm surge induced flood inundation for a 1-in-50-year return period.	Gridded data	Deltares global flood map (https://microsoft.github.io/AIforEarth DataSets/data/deltares-floods.html#global-datasets)
	Cyclone wind speed	Wind speed data from 1980 to 2022.	Gridded data	NOAA Regional and Mesoscale Meteorology Branch (RAMMB) (https ://rammb2.cira.colostate.edu/)
	Salinity intrusion	This indicator indicates the salinity intrusion in coastal areas.	Gridded data	http://earthexplorer.usgs.gov Bangladesh Agricultural Research Council (https://barc.gov.bd/)
	Precipitation intensity	Daily precipitation data from 2017 to 2022.	Gridded data	Precipitation Data (https://power.larc.nasa.gov/)
	Cyclone frequency	TC occurrences in coastal Bangladesh from 1960 to 2022.	Gridded data	International Best Track Archive for Climate Stewardship (IBTrACS) (htt ps://www.ncei.noaa.gov/products/international-best-track-archive)
Exposure	Population density	Number of people per grid cell.	Gridded data	WorldPop/Facebook (https://dataforgood.facebook.com/dfg/tools/high -resolution-population-density-maps)
	Proximity to cyclone track	Euclidean distance from cyclone track.	Gridded data	International Best Track Archive for Climate Stewardship (IBTrACS) (htt ps://www.ncei.noaa.gov/products/international-best-track-archive)
	Proximity to coastline	Euclidean distance from coastline.	Gridded data	Estimated from coastline data from WARPO (http://www.warpo.gov.bd/)
	Poverty	Wealth index value per grid cell.	Gridded data	Wealth Index data from https://hub.worldpop.org/geodata/summary? id=1274 Steele et al. (2017)
	Vulnerable age groups	Number of vulnerable people (male or female aged <15 or >65 years) per grid cell.	Gridded data	Age & sex structure Index data from WorldPop (https://hub.worldpop .org/project/categories?id=8)
Vulnerability	Elevation	Digital elevation model (DEM) at 30m spatial resolution.	Gridded data	Advanced Land Observation Satellite (ALOS) DEM (https://www.eorc .jaxa.jp/ALOS/en/aw3d30/data/index.html)
	Slope	Estimated using the DEM.	Gridded data	Estimated from DEM
	Drainage density	Drainage density per grid cell.	Gridded data	Estimated from DEM
	Distance to road networks	Euclidean distance to the existing road network.	Gridded data	Derived from Open Street Map (https://www.openstreetmap.org/#map=7/23.721/90.351)
	Built-up areas	Each grid cell indicates whether the land cover type is a built-up area or not.	Gridded data	Esri Global Land Cover Map (https://livingatlas.arcgis.com/landcover/)
Adaptive capacity	Distance to cyclone shelter	Euclidean distance to the existing cyclone shelters.	Map (geographical location)	GeoDASH (https://geodash.gov.bd/)
	Proximity to health facilities	Euclidean distance to the existing health facilities.	Map (geographical location)	Humanitarian Data Exchange (https://data.humdata.org/)
	Polders	Areas enclosed by coastal embankments.	Gridded data	Water Resources Planning Organisation (http://www.warpo.gov.bd/)
	Vegetation cover	Each grid cell indicates whether the land cover type is a vegetation cover or not.	Gridded data	Esri Global Land Cover Map (https://livingatlas.arcgis.com/landcover/)
	Employment density	Employment density value in each grid cell.	Gridded data	Humanitarian Data Exchange (https://data.humdata.org/)
	Education facilities	Number of education institution per grid cell.	Gridded data	Humanitarian Data Exchange (https://data.humdata.org/)

distinct regions: the stable deltaic western region, the deltaic central region, and the deltaic eastern region of the Pacific type, in accordance with data from the Bangladesh Bureau of Statistics. This region stands out for its intricate network of rivers, spanning a staggering 24,000 kilometers, including numerous islands scattered among the channels, a notable underwater canyon known as the Swatch of No Ground, a funnel-shaped segment of the northern Bay of Bengal, extensive debris transport, shallow terrain characterized by elevations ranging from 1.2 to 4.5 m above mean sea level, and the recurrent occurrence of formidable tropical cyclones (Hoque et al., 2017). Cyclones originating in the Bay of Bengal frequently make landfall along the coast of Bangladesh. Notably, the Meghna Estuary entrance, situated east of Bhola, experiences tidal ranges of up to 3 m, which may reach as high as 7 m further west. The coastal regions of Bangladesh also witness the most intense winds, with speeds of up to 220 kilometers per hour (Cai et al., 2020). The cyclone season in the Bay of Bengal primarily spans the pre-monsoon months of April through May and the post-monsoon months of October through November (Gori et al., 2022).

2.2. Assessing multi-hazard risk

This study delved into the assessment of multi-hazard risk induced by tropical cyclones (hereinafter TC) in coastal Bangladesh, considering a broad range of physical, social, and economic factors such as infrastructure, population density, poverty levels, and access to essential services. To evaluate the risk comprehensively, the study employed the following formula:

$$Risk = (Hazard \times Vulnerability \times Exposure) \,/\, Adaptive\ Capacity \quad (1)$$

where, hazard is the likelihood and magnitude of an extreme event triggered by a TC; vulnerability refers to the susceptibility of the population and/or assets to be impacted by multiple hazards; exposure quantifies the presence of resources or people in a hazardous location, and adaptive capacity denotes the region's ability to prepare for, manage, and recover from hazard-related effects. Raster layers depicting these risk components were generated using geographic information systems (GIS) and remote sensing-based data, as detailed in Table 1.

2.2.1. Hazard analysis

This study focused on four types of hazards associated with TC events in coastal Bangladesh: storm surge-induced flooding, salinity intrusion, extreme precipitation, and cyclonic winds. Storm surge-induced flood events are relatively common along the coastal areas of Bangladesh during TC events. Historical records indicate that several significant TC

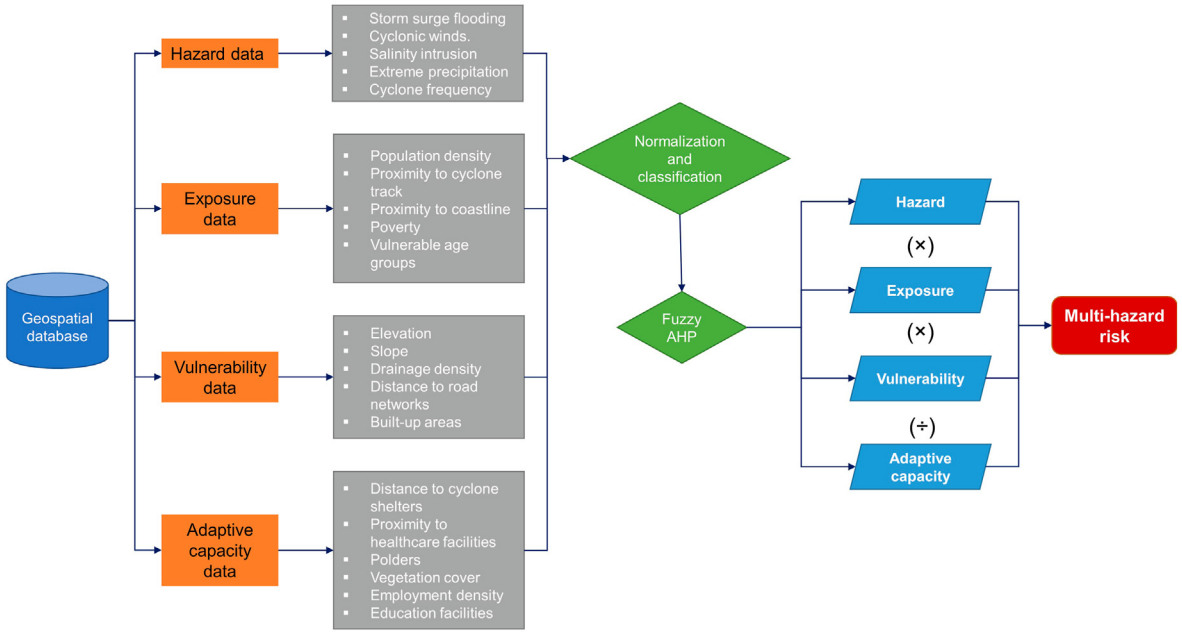

Fig. 1. Methodological flowchart of the study.

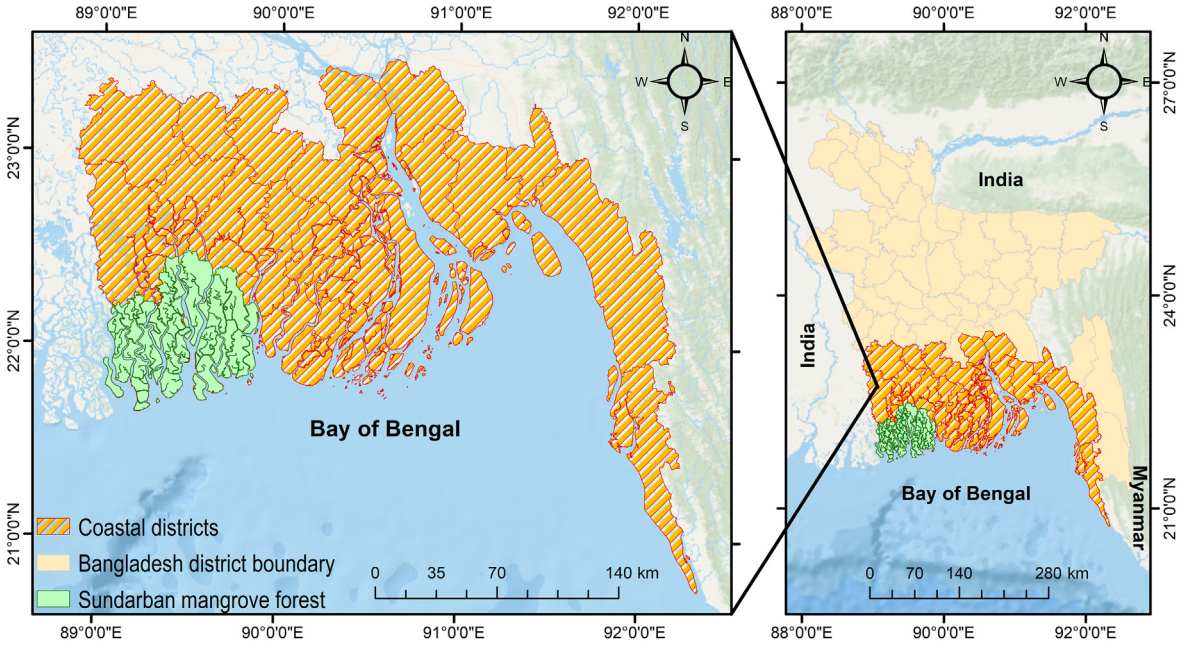

Fig. 2. The coastal region of Bangladesh.

events have led to coastal inundations due to storm surges. In this study, coastal flood inundation data was sourced from Deltares (https://www.deltares.nl/en). Specifically, a coastal flood event with a 1-in-50-year return period was considered, aligning with Bangladesh's coastal flood management policies, which address a similar flood magnitude. This dataset has a spatial resolution of 100 m (Fig. S1(a) in the supplementary document).

To create a 30-m raster layer depicting TC wind speed, wind speed data from 1980 to 2022 was collected from the NOAA Regional and Mesoscale Meteorology Branch (Fig. S1(b) in the supplementary document). Salinity intrusion data was generated using information obtained from the Bangladesh Agricultural Research Council (https://barc.gov.bd/) (Fig. S1(c) in the supplementary document). Finally, a raster layer representing precipitation intensity was created using data from NASA's Power Larc satellite (Fig. S1(d) in the supplementary document).

Using information from the International Best Track Archive for Climate Stewardship (IBTrACS), the study looked at the frequency of TC occurrences in coastal Bangladesh from 1960 to 2022. The main source for historical data on TC that affected coastal areas was this dataset, a thorough global archive of TC tracks and details. The study used structured digital formats to record the crucial details of cyclone occurrence, intensity, and tracks, including NetCDF. In order to shed light on the temporal and spatial patterns of cyclonic events in this vulnerable coastal area, the analysis set out to create a layer that represented cyclone frequency. In addition, the supporting document (Fig. S1(e)) probably includes illustrations to help explain the study's conclusions.

2.2.2. Exposure analysis

The exposure of an area to TC is influenced by various factors, including poverty level, proximity to cyclone track, proximity to coastline, population density, and vulnerable age group. The physical component of these factors was primarily considered for this study. With the population along shorelines growing rapidly worldwide, vulnerability levels can vary spatially due to population concentration and density. The study utilized WorldPop (https://www.worldpop.org/) population data to create the population density layer (Fig. S2 (a)). Proximity to the shore and cyclone path are crucial factors in evaluating cyclone exposure, with people and property closer to the coastlines and storm tracks being more susceptible to the effects of TCs. Coastal proximity data was obtained through measuring the distance between the study areas and the coastline using the Google Earth Pro ruler (Fig. S2 (c)). A raster layer of closeness to cyclone tracks was derived using the International Best Track Archive for Climate Stewardship (IBTrACS) data from 1968 to 2022 (www.ncdc.noaa.gov/ibtracs/), with the proximity analysis and creation of multi-ring buffers around cyclone tracks (Fig. S2 (b)). Poverty level is an important indicator for explaining exposure to TC. The study used the wealth index data from Steele et al. (2017) to consider poverty (Fig. S2 (d)). Lastly, we considered the vulnerable age group, including the population below 15 years old and above 65 years old, for exposure analysis. The layers of different age groups were added together, considering both male and female populations, to create the vulnerable age group layer (Fig. S2 (e)).

2.2.3. Vulnerability analysis

To estimate vulnerability to TC, five indicators were identified, including elevation, slope, drainage density, distance to road networks, and built-up area (Table 1). Elevation is associated with TC vulnerability, as areas with higher elevation correspond to lower level of vulnerability, and vice versa (Hoque et al., 2021). To derive a raster layer of elevation, Advanced Land Observing Satellite (ALOS) digital elevation model (DEM) data at 30m spatial resolution was used (Fig. S3 (a)). A quantile classification technique was employed in ArcGIS 10.8 to categorize the layer into five classes: very low, low, moderate, high, and very high. Like elevation, areas with higher slopes are less vulnerable to TC compared to areas with lower slopes. We derived a gridded slope layer utilizing the DEM data (Fig. S3 (b)). The DEM was further used to develop a layer of drainage density. Therefore, we extracted drainage streams and delineated drainage basins in the study area, following a methodology applied in Adnan et al. (2019a). The drainage density layer was classified using the quantile classification technique (Fig. S3 (c)). The location of an area from the existing road network could indicate the level vulnerability. With an increase in distance from road network, vulnerability tends to increase (Hoque et al., 2019). In this study, we utilized a road network from the Open Street Map to estimate the Euclidean distance of each location (of the study area) from the closest road (Fig. S3 (d)). The built-up area was the final indicator to define vulnerability. Cyclone vulnerability tends to increase with an increase in the extent of built-up area (Ehrlich et al., 2018). This study used the global landcover data from ESRI (Karra et al., 2021) to identify built-up areas (Fig. S3 (e)).

Table 2
Triangular fuzzy numbers for different variables.

Linguistic variable	Crisp number	Triangular fuzzy numbers	Reciprocal triangular fuzzy numbers
Equally strong	1	(1, 1, 1)	(1, 1, 1)
Intermediate	2	(1, 2, 3)	(1/3, 1/2, 1)
Moderately strong	3	(2, 3, 4)	(1/4, 1/3, 1/2)
Strong	5	(4, 5, 6)	(1/6, 1/5, 1/4)
Very strong	7	(6, 7, 8)	(1/8, 1/7, 1/6)
Extremely strong	9	(9, 9, 9)	(1/9, 1/9, 1/9)

Table 3
Weights of different indicators generated through the FAHP model using the TFN approach.

Multi-hazard indicators	Weight (%)	Exposure indicators	Weight (%)
Storm surge induced flood inundation	5.20	Poverty level	4.49
Cyclone wind speed	11.74	Proximity to cyclone track	10.25
Salinity Intrusion	16.12	Proximity to coastline	18.67
Precipitation intensity	29.34	Population density	30.04
Cyclone Frequency	37.60	Vulnerable age group	36.55
Vulnerability indicators	**Weight (%)**	**Adaptive capacity indicators**	**Weight (%)**
Elevation	6.18	Distance to cyclone shelter	4.49
Slope	8.82	Proximity to health facilities	6.03
Drainage Density	17.18	Education facilities	10.28
Density of road networks	30.37	Employment density	20.78
Land use and Land cover	37.45	Polder	24.10
		Vegetation Cover	34.31

2.2.4. Analyzing adaptive capacity

This study considered six adaptive capacity indicators — distance to cyclone shelter, proximity to health facilities, education facilities, employment density, polder presence, and vegetation cover — that have potential to mitigate cyclone induced multi-hazard risk. Location data of cyclone shelters were collected from the GeoDASH (https://geodash.gov.bd/). The locations of healthcare facilities were obtained from the Humanitarian Data Exchange (https://data.humdata.org/), which also provides data for education facilities and employment density. The 'Euclidian distance' technique was employed to derive spatial layers of distance to cyclone shelters and healthcare facilities. These two indicators are negatively correlated with adaptive capacity as vulnerability of an area to cyclones tends to increase with an increase in distance from cyclone shelters and healthcare facilities. Data on areas enclosed by polders (i.e., coastal embankments) were collected from the Water Resources Planning Organization (WARPO) (http://www.warpo.gov.bd/). A layer of vegetation cover was extracted from the ESRI global land cover data. Four indicators such as education facilities, employment density, presence of polders, and vegetation cover are positively associated with adaptive capacity. An increase in the corresponding values of these indicators increases the probability of an area adapting to the adverse impacts of cyclones. The maps of all six indicators of adaptive capacity are illustrated in Fig. S4 of supplementary document.

2.3. Fuzzy Analytic hierarchy process (FAHP)

In this study, a combination of the Fuzzy Analytic Hierarchy Process (FAHP) and triangulation techniques was employed to determine the weights of various indicators associated with multi-hazard risk. The FAHP method was chosen over the traditional Analytic Hierarchy Process (AHP) to address issues related to unbalanced judgment scales and the precise handling of inherent uncertainties and vagueness that arise from the AHP method (Yang et al., 2013). While various FAHP techniques exist, this study utilized an integrated FAHP technique as proposed by Chang (1996). This technique simplifies the pairwise comparison by employing triangular fuzzy numbers (TFNs), thereby alleviating the need for cumbersome comparison processes. The methodology used for generating weights for the indicators of multi-hazard risk encompassed several key steps. Initially, raster layers of all indicators within the different components of risk (i.e., hazard, exposure, vulnerability, and adaptive capacity) were standardized using the following equation:

$$x_i' = \frac{x_i - min(x)}{max(x) - min(x)} \quad (2)$$

where i denotes factors associated with various components of risk, x' is the transformed value ranges between 0 and 1 and x is the original value. Following this, all normalized raster layers were recategorized into five classes (1–5) using the Jenks natural break algorithm (Jenks, 1967), with 1 denoting 'very low' and 5 indicating 'very high'. This iterative classifier, known for minimizing inter-cluster variance, has been widely adopted in recent risk assessment studies (Deroliya et al., 2022).

Next, matrices for pairwise comparisons were constructed using the geometric mean approach, integrating the input from six experts based on the relative relevance of the chosen criteria. The judgments of experts and decision-makers play a critical role in determining the importance of these criteria in the context of the geographical problem. Several linguistic factors were utilized as qualitative representations of these judgments, and to quantify these decisions appropriately, a fuzzy set was employed. For this study, verbal factors were translated into quantitative values using a triangular fuzzy set. These pairwise comparison matrices were then combined and synthesized in the third step to create a set of overall priorities within the hierarchy.

The consistency ratio (CR) was computed in the fourth step to validate the expert ratings in the pairwise matrices. A CR value of 0.1 or lower was considered indicative of accurate judgments. The CR was determined using the following equation:

$$CR = \frac{Consistency\ Index}{Random\ Index} \tag{3}$$

where, the matrix order (n) supplied by the Saaty scale creator is used to generate the random index (RI). Additionally, the following equation was employed to establish the consistency index (CI):

$$CI = \frac{\delta_{max} - n}{n-1} \tag{4}$$

where, δ_{max} and n denote the biggest eigenvalue and order of a matrix, respectively.

Finally, Table 2 was utilized to convert pairwise matrix criterion weights into linguistic variables. The approach outlined by Chang (1996) was applied to determine priority weights. The resulting weights for the multi-hazard risk indicators are presented in Table 3.

3. Results and discussion

3.1. Multi-hazard prone areas

Fig. 3 (a) represents an integrated map of five distinct hazards (i.e., storm surge-induced flooding, salinity intrusion, heavy precipitation, cyclonic winds, and cyclone frequency) associated with TCs in the coastal region of Bangladesh. The study has revealed that a significant portion of the study area was susceptible to multiple hazards, with approximately 47.3% of the area falling within the moderate to very high multi-hazard prone zone. Conversely, the remaining areas were situated within relatively low (low and very low) hazard-prone zones. Notably, the southeastern and southwestern coasts of Bangladesh exhibited significant susceptibility to TC-induced multi-hazard events. District-wise distribution of these hazard prone areas is illustrated in Fig. 4 (a). Southeastern districts, such as Cox's Bazar, Feni, and Chittagong, as well as southwestern districts like Khulna, Satkhira, and Barguna, featured multi-hazard prone areas of 'high' and 'very high' severity. Notably, the northwestern part of Cox's Bazar district and certain sections of Ukhia and Teknaf sub-districts were identified as highly multi-hazard prone

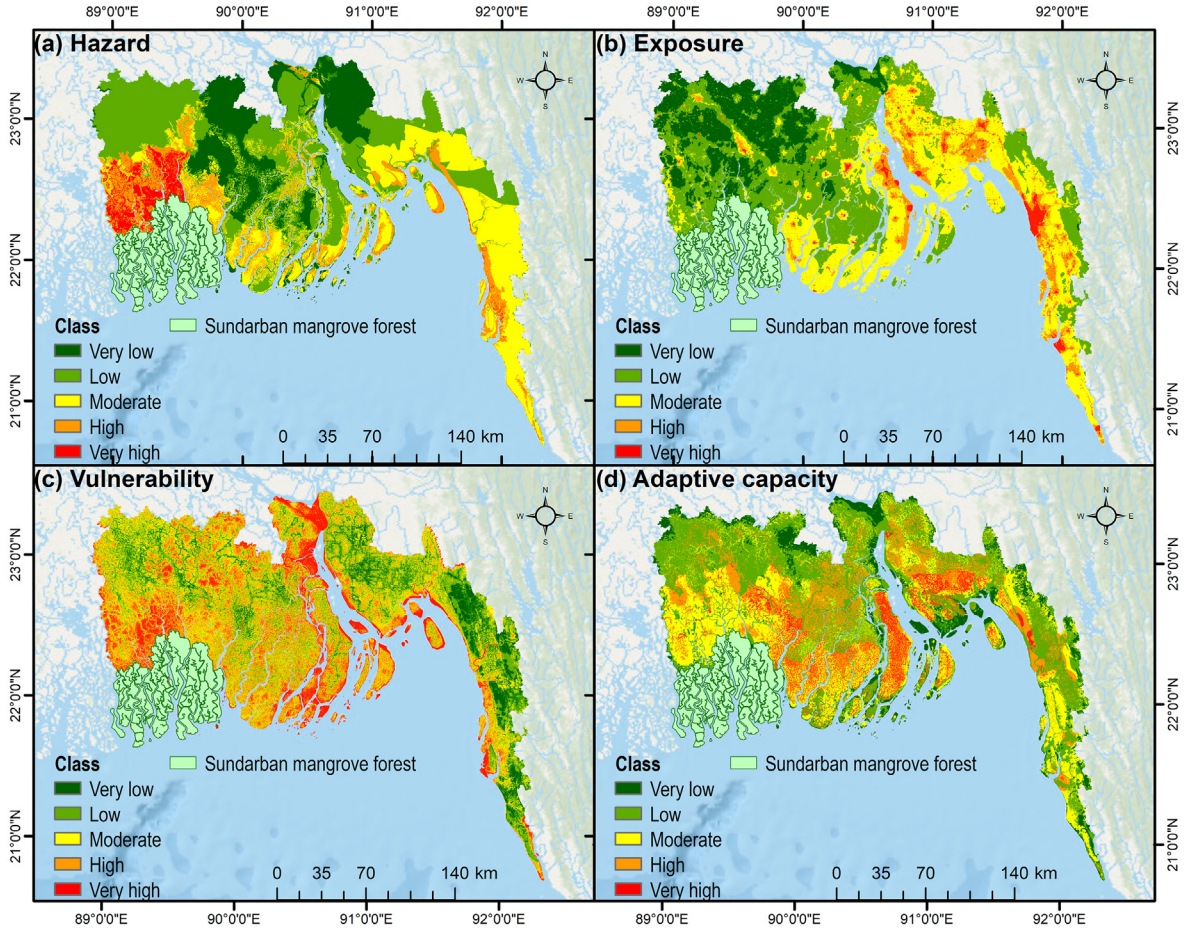

Fig. 3. Components of risk: (a) Hazard, (b) Exposure, (c) Vulnerability, and (d) Adaptive Capacity.

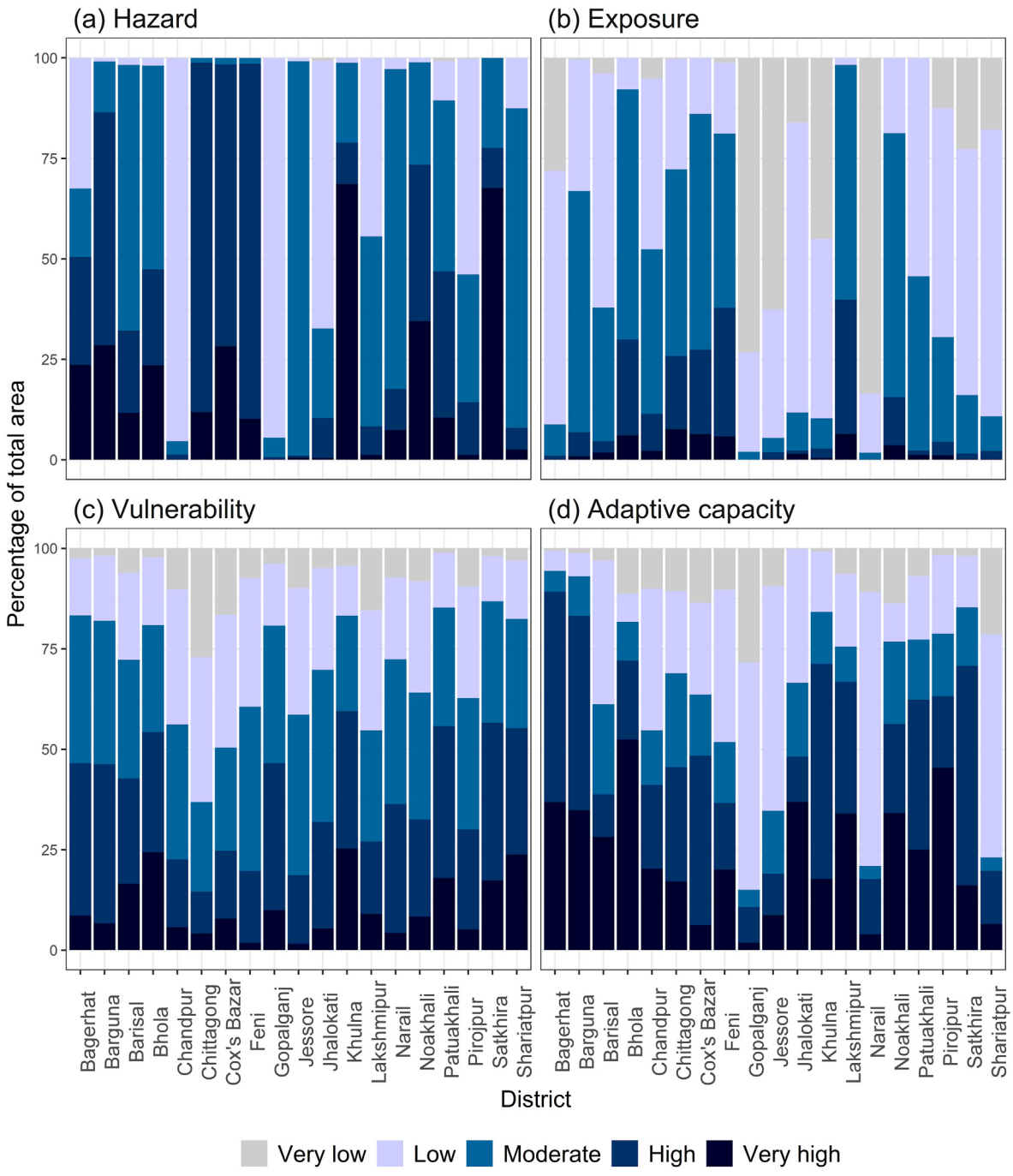

Fig. 4. District wise distribution of risk components: (a) Hazard; (b) Exposure (c) Vulnerability (d) Adaptive Capacity.

areas. These highly vulnerable areas encompass Rohingya Refugee camps.

3.2. Exposure to multi-hazard events

This study quantifies the extent of areas exposed to multi-hazard events associated with TCs, as depicted in Fig. 3 (b). Approximately 71% of the entire coastal region of Bangladesh was found to be exposed to TC-induced multi-hazard events, ranging from 'moderate' to 'very high' severity. In contrast, the remaining 29% of the area exhibited a lower level of exposure. Particular attention was paid on estimating exposure for the population residing in multi-hazard prone areas, including vulnerable age groups (aged <15 or >65 years).

Lakshmipur district exhibited the highest level of exposure, with 98% of its total area exposed to multi-hazard events induced by TCs, ranging from 'moderate' to 'very high' severity. Closely following, approximately 92% of Bhola district's total area was found to be exposed. Other coastal districts with notably high exposure rates included Cox's Bazar (86%), Noakhali (81%), Feni (81%), Chittagong (72%), and Barguna (67%), as illustrated in Fig. 4 (b). It is noteworthy that, despite the southwest coast falling within a highly hazard-prone zone, the population density in this region is relatively low due to the presence of the Sundarbans Mangrove Forest, resulting in relatively lower exposure.

3.3. Vulnerable areas to multi-hazard events

Vulnerability within the coastal region of Bangladesh to TC-induced multi-hazard events was assessed in relation to various topographical

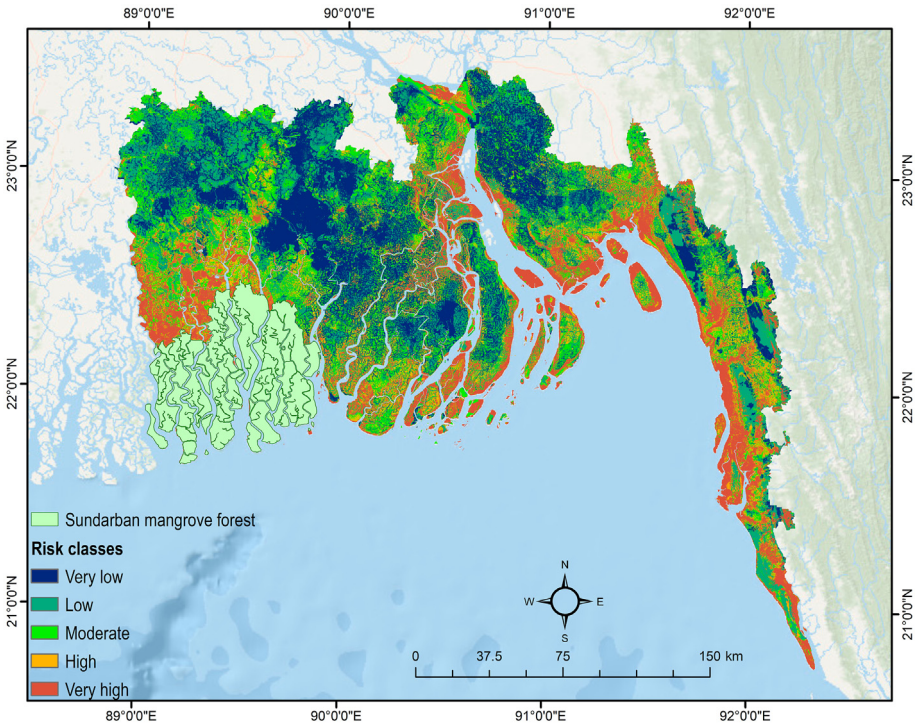

Fig. 5. Overall risk associated with multi-hazard events induced by tropical cyclone.

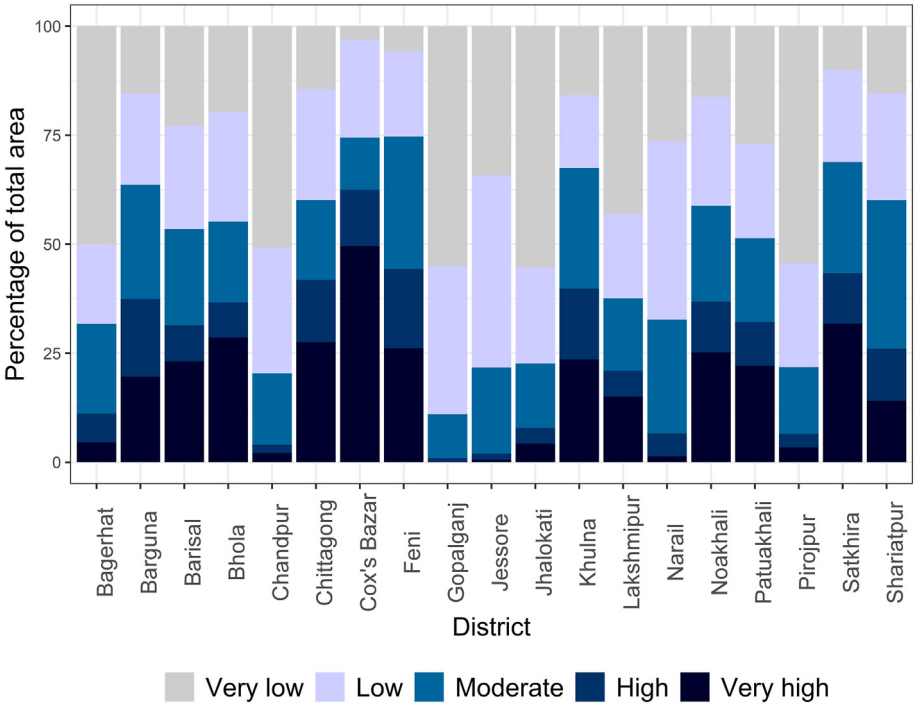

Fig. 6. Distribution of TC-induced multi-hazard risk-prone areas at district level.

and built-environmental factors, as outlined in Table 1. About 71% of the study area was classified as vulnerable to multi-hazard events of 'moderate' to 'very high' severity (Fig. 3 (c)). Notably, the southwestern and southcentral coasts exhibited particularly high vulnerability levels, primarily due to their locations in low-lying floodplain zones. With the exception of Chittagong district, situated in the southeastern coast of Bangladesh, more than 50% of the total area in all other districts were classified as vulnerable to multi-hazard events. Satkhira district emerged as the most vulnerable district, with 87% of its area identified as vulnerable, as illustrated in Fig. 4 (c).

3.4. *Areas with potential for multi-hazard adaptation*

This study assessed the adaptive capacity of the coastal region of Bangladesh, taking into account factors such as the proximity of an area to cyclone shelters and health facilities, education facilities, employment

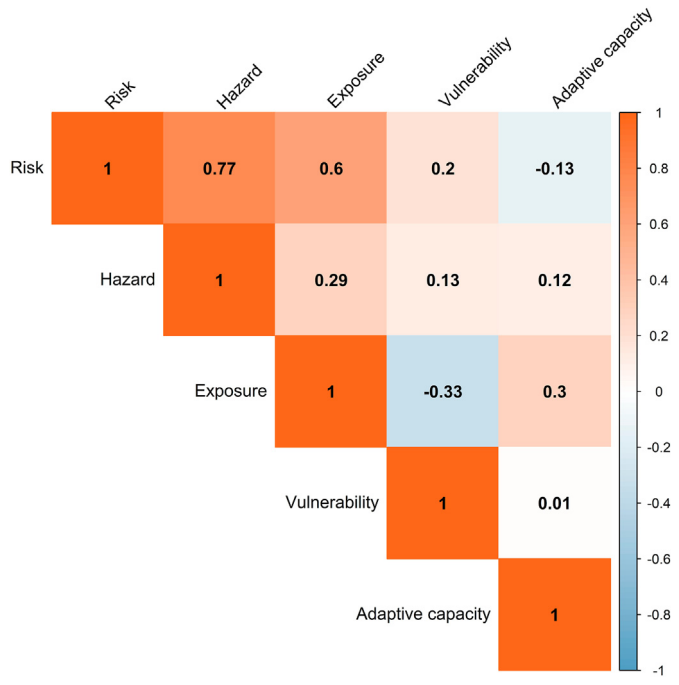

Fig. 7. Correlation between risk and its components (i.e., hazard, exposure, vulnerability, and adaptive capacity).

density, the presence of polders, and the extent of vegetation cover. The findings reveal that only 19.7% of the total area exhibited 'high' to 'very high' adaptive capacity in the face of cyclone-induced multi-hazard impacts, as illustrated in Fig. 3 (d). Areas in close proximity to critical facilities, including hospitals, cyclone shelters, and those equipped with effective warning systems, displayed a greater potential to withstand multi-hazard impacts. However, a substantial area, covering 27.6%, situated near and slightly inland from the coastline, was identified as possessing a moderate capability for mitigating cyclone impacts. This zone included sections of Teknaf, Sandwip, Chakaria, Kutubdia, Maheshkhali Cox Bazar, and Kutubdia. Furthermore, areas with low and extremely low mitigation capability, constituting 52.7% of the total area, were observed along the eastern and southernmost edges of the research site. Notably, these areas encompass the Rohingya refugee camps.

3.5. Multi-hazard risk prone areas

This study developed a comprehensive multi-hazard risk map of coastal Bangladesh by overlaying hazard, exposure, vulnerability, and adaptive capacity maps, using a weighted overlay approach. The resultant risk map was also classified into five categories, ranging from 'very low' to 'very high' risk prone zones. The results revealed that over 50% of the coastal region was located within the multi-hazard risk-prone category of 'moderate' to 'very high' intensity. The remaining 46.1% classified as low to very low risk-prone zones, as illustrated in Fig. 5.

The risk map was further subdivided at the district level to identify the most risk prone district (Fig. 6). More than 50% of the total area in 11 (out of 19) coastal districts was identified as being risk prone to cyclone-induced multi-hazard events. Geographically, districts located in the southeastern coasts and along the Meghna River estuary were found to be at high risk. The highest proportion of risk prone areas was found in southeastern districts Feni and Cox's Bazar, with 'moderate' to 'very high' risk prone areas encompassing 74.7% and 74.4% of the total area, respectively. Contrarily, inland districts were located within relatively low risk prone areas. For example, the lowest proportion of risk prone areas was estimated in Gopalganj district, with 11% of its total area being risk prone areas of 'moderate' to 'very high' severity.

This study further examined the correlation between multi-hazard risk and its components. In general, hazard, exposure, and vulnerability exhibited a positive association with the risk, while negative correlation was found with adaptive capacity. The strongest correlation was observed between risk and hazard, with a correlation coefficient of 0.77, followed by exposure at 0.6, and vulnerability at 0.2. Despite a negative association between risk and adaptive capacity, the correlation coefficient was very low at −0.13 (Fig. 7).

3.6. Contributions of associated hazards to multi-hazard risk

This study reveals a significant correlation between multi-hazard risk and the hazard component (section 3.5). To elucidate the spatial distribution of multi-hazard risk, the contributions of five distinct hazards associated with TC events were analyzed.

3.6.1. Storm surge induced flood inundation

Storm surges exert the most substantial influence on TC events, leading to the inundation of coastal regions. These surges are driven by the low-pressure systems generating high wind speeds. This study's estimation indicated that approximately 55% of the entire coastal region was susceptible to storm surge-induced flooding of 'moderate' to 'very high' severity (Fig. 8a). Notably, the southwestern and south-central coastal regions were particularly prone to inundation. A significant proportion of flood-prone areas were concentrated in districts such as Khulna, Barguna, Patuakhali, and Barisal (Fig. 9).

3.6.2. Salinity intrusion

TC events can induce salinity intrusion in coastal Bangladesh, primarily through storm surges and tidal waves (Miah et al., 2020). The present study identified a significant portion of the coastal region as prone to salinity intrusion. Fig. 8 (b) demonstrates that areas along the coastline are particularly vulnerable, with approximately 57% of the total area experiencing soil salinity of 'moderate' to 'very high' severity. Districts in the southwest and south-central coasts were especially susceptible, with more than 50% of the total area in 10 coastal districts prone to salinity intrusion. Barguna exhibited the highest levels, with nearly 80% of its total area indicating 'moderate' to 'very high' salinity levels. Other districts with pronounced salinity presence included Satkhira, Noakhali, Feni, Khulna, Lakshmipur, Shariatpur, Patuakhali, Cox's Bazar, and Bhola.

3.6.3. Extreme precipitation

TC events often result in extreme precipitation, leading to various flood events such as pluvial and flash flooding, along with landslides. For instance, TC 'Fani,' with a maximum gust speed of 180 km/h, brought an average daily precipitation of 150–300 mm/day (Kumar et al., 2020). This study revealed that over 50% of the coastal region of Bangladesh was susceptible to extreme precipitation resulting from TC events. Districts in the southeast and south-central coasts were at high risk of extreme precipitation events (Fig. 8 (c)). Out of the 19 coastal districts, more than 50% of the total area in 11 districts experienced a risk of moderate to very high severity from extreme precipitation. Cox's Bazar district was the most at-risk, with 94.8% of its area located within the 'moderate' to 'very high' risk zone. However, the lowest risk to extreme precipitation was observed in Jessore district (Fig. 9 (c)).

3.6.4. High wind speed

Winds associated with TC events can have detrimental effects on the natural and anthropogenic environments. For example, TC 'Fani' brought a maximum wind speed of 180 km/h, impacting human life, property, and assets (Kumar et al., 2020). This study identified areas highly susceptible to wind effects during TC events. Fig. 8 (d) indicates that a significant portion of the south-central and southeastern coastal zones were highly prone to wind effects. Approximately 58% of the total coastal region was estimated to be prone to wind effects of 'moderate' to 'very high' severity. Cox's Bazar and Feni districts were the most wind-prone

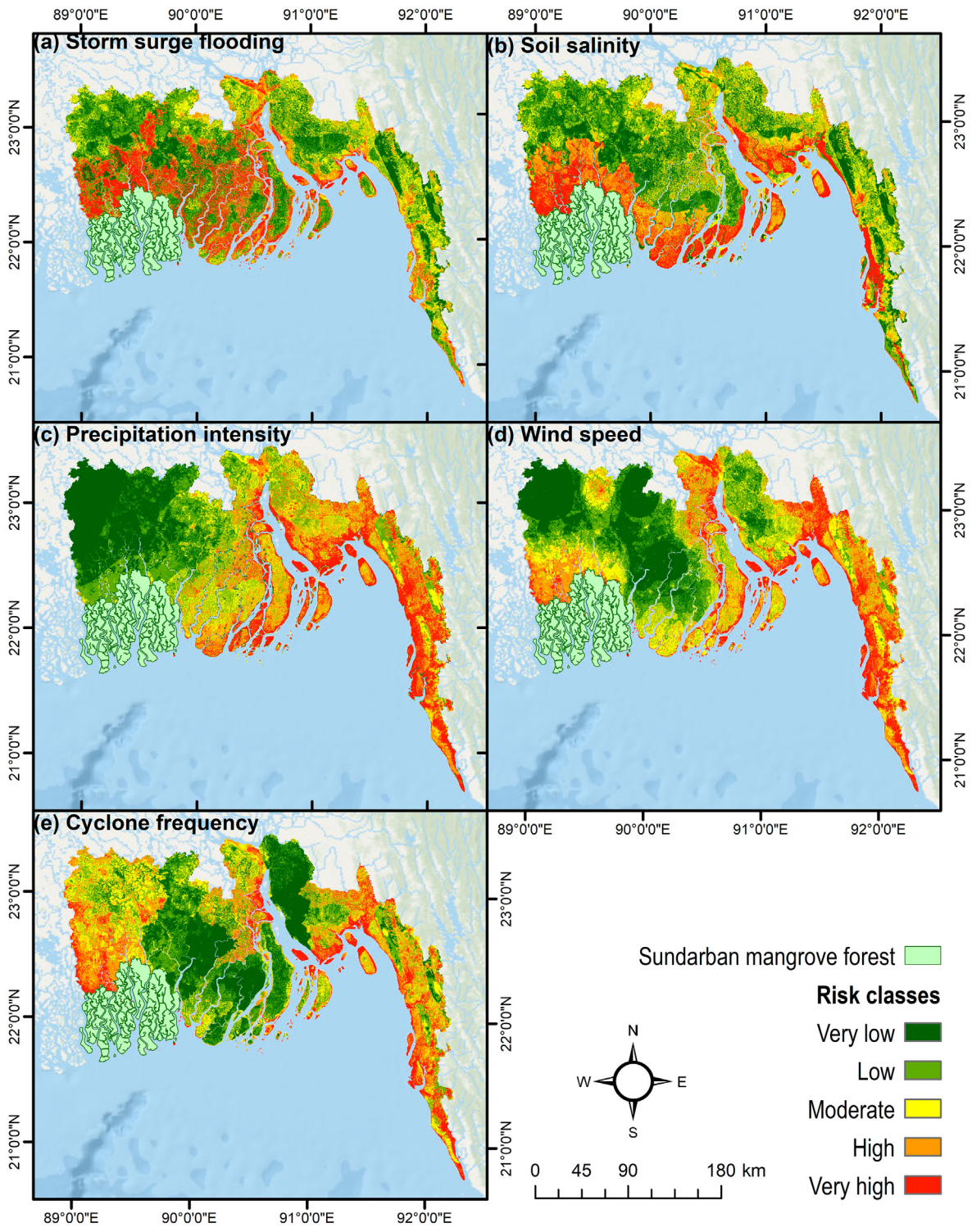

Fig. 8. Risks associated with five different types of associated hazards: (a) storm surge flooding (b) soil salinity (c) precipitation intensity (d) wind speed (e) cyclone frequency.

areas, with about 99% of their total areas at risk of 'moderate' to 'very high' severity. Conversely, relatively fewer wind impacts were observed in southwestern coastal districts.

3.6.5. *Frequency of TC*

Finally, TC-induced multi-hazard risk is linked to the frequency of TC events (Sahoo and Bhaskaran, 2018). This study estimated the risk associated with TC frequencies. The results indicated that about 55% of the total coastal region was at risk of frequent TC events of 'moderate' to 'very high' severity. Both the southwestern and southeastern regions were highly risk-prone zones (Fig. 8 (e)). More than 50% of the total area in 10 coastal districts was at risk of 'moderate' to 'very high' severity. Satkhira district was identified as the most risk-prone district, with over 95% of its area at risk of frequent TC events (Fig. 9 (e)).

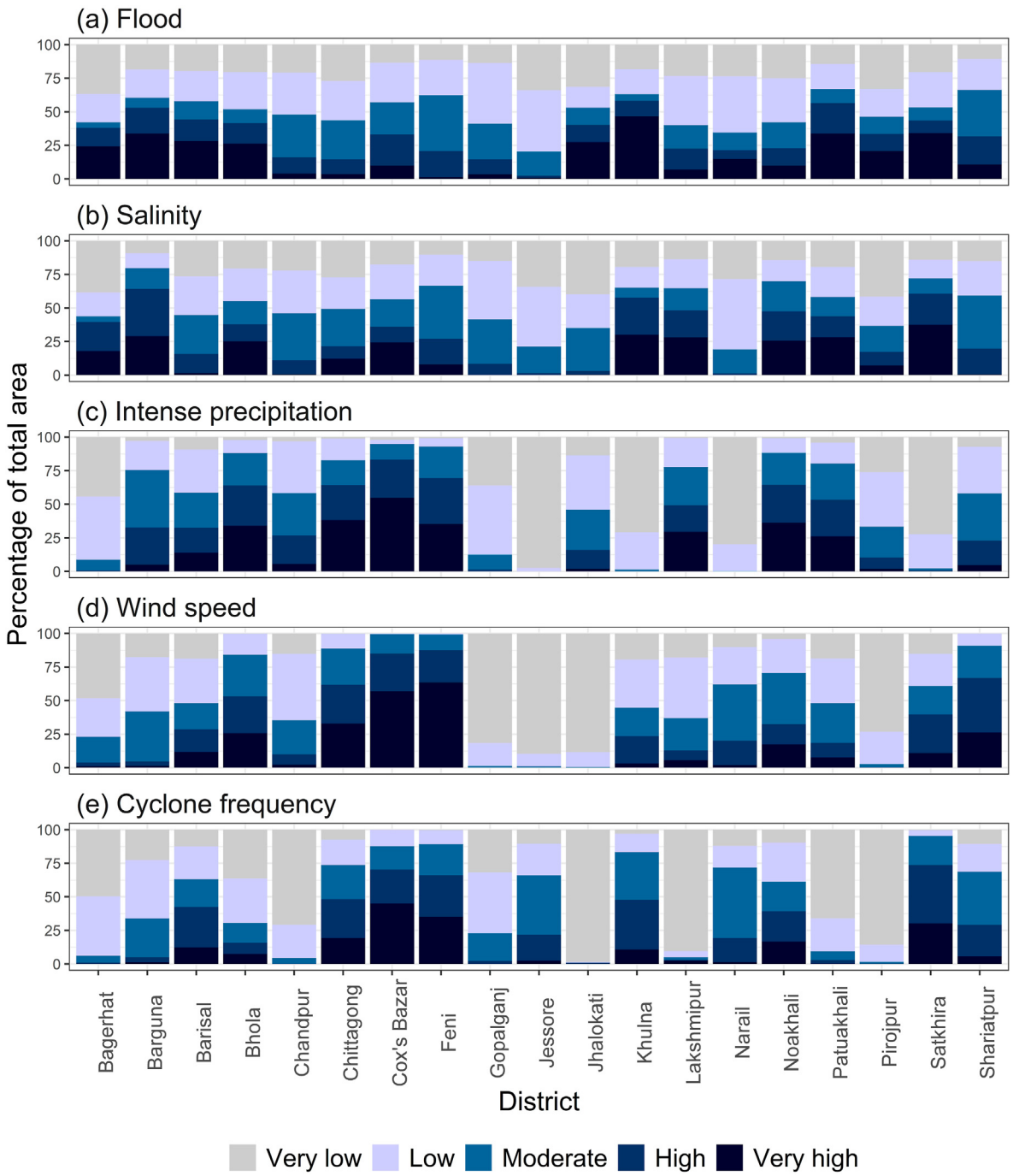

Fig. 9. District wise distribution of Tropical Cyclone induced multi-hazard risk assessment of: (a) Storm surge induced flood inundation (b) Salinity (c) precipitation intensity (d) wind speed (e) Cyclone frequency.

4. Discussion

This study aims to investigate the multi-hazard risks associated with tropical cyclone (TC) events in the coastal region of Bangladesh, using the Fuzzy Analytic Hierarchy Process (FAHP) model. Risk was assessed based on hazard, exposure, vulnerability, and mitigation capabilities within the study area. The findings indicate that over 50% of the region is prone to multi-hazard risks, with variations observed among different coastal districts. Cox's Bazar and Feni were identified as the most risk-prone districts.

Different risk components, including hazard, exposure, vulnerability, and mitigation capabilities, exerted varying degrees of influence on overall risk. Hazard, exposure, and vulnerability were positively correlated with risk, while adaptive capacity showed a negative association. The most significant correlation was identified with the hazard component, followed by exposure, vulnerability, and adaptive capacity. Similar associations were found in existing studies (Hoque et al., 2019). This study revealed that highly exposed and extremely vulnerable areas to TC-induced multi-hazard events experienced a high frequency of hazards, aligning with previous research (Hoque et al., 2019; Islam et al., 2016).

In terms of individual risk components, a substantial portion of coastal Bangladesh is susceptible to TC-induced multi-hazard events. The contributions of five associated hazards differ, with storm surge-induced flood events posing the highest impact on the coastal region, followed by intense precipitation. These associated hazards exhibit distinct

geographical variations. For example, districts such as Khulna, Barguna, Patuakhali, and Barisal, characterized by low-lying floodplains (with a mean elevation of 3.5m) and tidal rivers, were highly prone to storm surge-induced flooding. Land subsidence is a common phenomenon in these areas (Brown and Nicholls, 2015), which leads to surface depressions that are particularly vulnerable to inundation (Adnan et al., 2020). These regions are enclosed by coastal embankments, known as polders, although several recent studies have highlighted the limitations of these embankments in withstanding storm surge-induced flooding (Adnan et al., 2019b; Haque and Nicholls, 2018).

Concerning other associated hazards, this study found that areas along the coastline are highly prone to salinity intrusion, consistent with recent studies (Ashrafuzzaman et al., 2022; Miah et al., 2020). About 50% of the study area received extreme precipitation during TC events. Such heavy precipitation results in landslides, particularly in the hilly southeastern region (Fakhruddin et al., 2022). While the precipitation intensity in the southwestern coast is relatively low, its impact on flooding is significant. Adnan et al. (2019b) reported that the geomorphological changes brought about by the construction of polders have made the embanked region extremely prone to pluvial flooding, especially during TC events. In the case of extreme wind, southwestern coastal is relatively less prone to this hazard. The presence of the Sundarbans Mangrove Forest may be a contributing factor, as during various major historical TC events, the forest acted as a natural buffer (Akber et al., 2018). However, the most frequent TC landfall occurred in southwest coastal district Satkhira. This district was severely affected by various historical TC events (Salman, 2023).

Exposure analysis revealed that a significant population, particularly those aged below 15 or over 65 years, was exposed to multi-hazard events. Underdeveloped and densely populated areas, particularly on the eastern coast, were identified as highly exposed areas. In the southwestern coast, the presence of highly vegetated areas such the Sundarban Mangrove Forest could be associated with relatively low level of exposure to multi-hazard events (Akber et al., 2018). Areas in proximity to critical infrastructure, such as hospitals, cyclone shelters, and those equipped with effective warning systems, displayed a greater potential to withstand multi-hazard impacts. Adshead et al. (2023) emphasized the importance of locating critical infrastructure, like cyclone shelters, within short distances to all settlements for effectiveness. According to Chen et al. (2018), people living close to hospitals and other public facilities receive essential services and support, making them less prone to risks in a multi-hazard environment.

5. Conclusion

In conclusion, this study employed the Fuzzy Analytic Hierarchy Process (FAHP) model to comprehensively investigate multi-hazard risks associated with tropical cyclone (TC) events in the coastal region of Bangladesh. The findings revealed that over 50% of the region is susceptible to multi-hazard risks, displaying variations among different coastal districts. The study underscored that areas highly exposed and extremely vulnerable to TC-induced multi-hazard events are subject to a high frequency of hazards, with storm surge-induced flood events having the most significant impact on the coastal region. Exposure analysis highlighted substantial populations, especially vulnerable age groups, and underdeveloped areas, underscoring the critical role of proximity to essential infrastructure for enhancing resilience.

While providing valuable insights, this study has certain limitations that need consideration. The reliance on secondary data sources implies that the accuracy of the results depends on the precision of these datasets. Additionally, the use of wealth index data from 2010, due to the unavailability of the latest gridded poverty data, introduces a temporal limitation. Moreover, the FAHP model may be susceptible to subjective bias. Despite these limitations, this study addresses a significant gap in the existing literature by quantifying risks through a multi-hazard approach. The proposed framework and obtained results offer potential guidance for the development of multi-hazard risk mitigation policies in coastal Bangladesh and other regions with similar contexts. Furthermore, this study lays the groundwork for future research aimed at constructing high-resolution multi-hazard risk models.

CRediT authorship contribution statement

Sajib Sarker: Writing – original draft, Visualization, Software, Methodology, Formal analysis, Data curation. **Mohammed Sarfaraz Gani Adnan:** Validation, Supervision, Resources, Methodology, Investigation, Conceptualization, Visualization, Writing – review & editing.

Declaration of competing interest

The authors declare that they have no known competing financial interests or personal relationships that could have appeared to influence the work reported in this paper.

Appendix A. Supplementary data

Supplementary data to this article can be found online at https://doi.org/10.1016/j.nhres.2023.11.007.

References

Adnan, M.S.G., Dewan, A., Zannat, K.E., Abdullah, A.Y.M., 2019a. The use of watershed geomorphic data in flash flood susceptibility zoning: a case study of the Karnaphuli and Sangu river basins of Bangladesh. Nat. Hazards 99, 425–448.
Adnan, M.S.G., Haque, A., Hall, J.W., 2019b. Have coastal embankments reduced flooding in Bangladesh? Sci. Total Environ. 682, 405–416.
Adnan, M.S.G., Talchabhadel, R., Nakagawa, H., Hall, J.W., 2020. The potential of tidal river management for flood alleviation in south western Bangladesh. Sci. Total Environ. 731, 138747.
Adshead, D., Paszkowski, A., Gall, S.S., Peard, A.M., Adnan, M.S.G., Verschuur, J., Hall, J., 2023. Climate Threats to Coastal Infrastructure and Sustainable Development Outcomes.
Aguirre-Ayerbe, I., Merino, M., Aye, S.L., Dissanayake, R., Shadiya, F., Lopez, C.M., 2020. An evaluation of availability and adequacy of Multi-Hazard Early Warning Systems in Asian countries: a baseline study. Int. J. Disaster Risk Reduc. 49, 101749.
Akay, H., 2021. Spatial modeling of snow avalanche susceptibility using hybrid and ensemble machine learning techniques. Catena 206, 105524.
Akber, M.A., Patwary, M.M., Islam, M.A., Rahman, M.R., 2018. Storm protection service of the Sundarbans mangrove forest, Bangladesh. Nat. Hazards 94, 405–418.
Alam, E., Collins, A.E., 2010. Cyclone disaster vulnerability and response experiences in coastal Bangladesh. Disasters 34, 931–954.
Anwar, G.A., Dong, Y., Li, Y., 2020. Performance-based decision-making of buildings under seismic hazard considering long-term loss, sustainability, and resilience. Structure and Infrastructure Engineering 17, 454–470.
Argyroudis, S.A., Mitoulis, S.A., Hofer, L., Zanini, M.A., Tubaldi, E., Frangopol, D.M., 2020. Resilience assessment framework for critical infrastructure in a multi-hazard environment: case study on transport assets. Sci. Total Environ. 714, 136854.
Ashrafuzzaman, M., Artemi, C., Santos, F.D., Schmidt, L., 2022. Current and future salinity intrusion in the south-western coastal region of Bangladesh. Spanish Journal of Soil Science 12, 10017.
Bakkensen, L.A., Mendelsohn, R.O., 2019. Global Tropical Cyclone Damages and Fatalities under Climate Change: an Updated Assessment. Hurricane Risk, pp. 179–197.
Barbour, E.J., Adnan, M.S.G., Borgomeo, E., Paprocki, K., Khan, M.S.A., Salehin, M., Hall, J.W., 2022. The unequal distribution of water risks and adaptation benefits in coastal Bangladesh. Nat. Sustain. 5, 294–302.
Bera, R., Maiti, R., 2021. Multi hazards risk assessment of Indian Sundarbans using GIS based Analytic Hierarchy Process (AHP). Regional Studies in Marine Science 44, 101766.
Bernal, G.A., Salgado-Gálvez, M.A., Zuloaga, D., Tristancho, J., González, D., Cardona, O.-D., 2017. Integration of probabilistic and multi-hazard risk assessment within urban development planning and emergency preparedness and response: application to Manizales, Colombia. International Journal of Disaster Risk Science 8, 270–283.
Bianchi, E., Malki-Epshtein, L., 2021. Evaluating the risk to Bangladeshi coastal infrastructure from tropical cyclones under climate change. Int. J. Disaster Risk Reduc. 57, 102147.
Bourdeau-Brien, M., Kryzanowski, L., 2020. Natural disasters and risk aversion. J. Econ. Behav. Organ. 177, 818–835.
Brown, S., Nicholls, R.J., 2015. Subsidence and human influences in mega deltas: the case of the Ganges–Brahmaputra–Meghna. Sci. Total Environ. 527, 362–374.
Cai, L., Li, Y., Chen, M., Zou, Z., 2020. Tropical cyclone risk assessment for China at the provincial level based on clustering analysis. Geomatics, Nat. Hazards Risk 11, 869–886.

Chang, D.-Y., 1996. Applications of the extent analysis method on fuzzy AHP. Eur. J. Oper. Res. 95, 649–655.
Chen, W., Zhai, G., Ren, C., Shi, Y., Zhang, J., 2018. Urban resources selection and allocation for emergency shelters: in a multi-hazard environment. Int. J. Environ. Res. Publ. Health 15, 1261.
Choi, E., Ha, J.-G., Hahm, D., Kim, M.K., 2021. A review of multihazard risk assessment: progress, potential, and challenges in the application to nuclear power plants. Int. J. Disaster Risk Reduc. 53, 101933.
Cutter, S.L., Finch, C., 2008. Temporal and spatial changes in social vulnerability to natural hazards. Proc. Natl. Acad. Sci. USA 105, 2301–2306.
Dasgupta, S., Huq, M., Khan, Z.H., Ahmed, M.M.Z., Mukherjee, N., Khan, M.F., Pandey, K., 2014. Cyclones in a changing climate: the case of Bangladesh. Clim. Dev. 6, 96–110.
de Brito, M.M., Evers, M., 2016. Multi-criteria decision-making for flood risk management: a survey of the current state of the art. Nat. Hazards Earth Syst. Sci. 16, 1019–1033.
Deroliya, P., Ghosh, M., Mohanty, M.P., Ghosh, S., Rao, K.D., Karmakar, S., 2022. A novel flood risk mapping approach with machine learning considering geomorphic and socio-economic vulnerability dimensions. Sci. Total Environ. 851, 158002.
Ehrlich, D., Melchiorri, M., Florczyk, A.J., Pesaresi, M., Kemper, T., Corbane, C., Freire, S., Schiavina, M., Siragusa, A., 2018. Remote sensing derived built-up area and population density to quantify global exposure to five natural hazards over time. Rem. Sens. 10, 1378.
Eshrati, L., Mahmoudzadeh, A., Taghvaei, M., 2015. Multi hazards risk assessment, a new methodology. International Journal of Health System and Disaster Management 3, 79.
Fakhruddin, B., Kintada, K., Hassan, Q., 2022. Understanding hazards: probabilistic cyclone modelling for disaster risk to the Eastern Coast in Bangladesh. Progress in disaster science 13, 100216.
Gill, J.C., Duncan, M., Ciurean, R., Smale, L., Stuparu, D., Schlumberger, J., de Ruiter, M., Tiggeloven, T., Torresan, S., Gottardo, S., 2022. D1. 2 Handbook of Multi-Hazard, Multi-Risk Definitions and Concepts.
Gill, J.C., Malamud, B.D., 2014. Reviewing and visualizing the interactions of natural hazards. Rev. Geophys. 52, 680–722.
Gill, J.C., Malamud, B.D., 2016. Hazard interactions and interaction networks (cascades) within multi-hazard methodologies. Earth System Dynamics 7, 659–679.
Gill, J.C., Malamud, B.D., 2017. Anthropogenic processes, natural hazards, and interactions in a multi-hazard framework. Earth Sci. Rev. 166, 246–269.
Girishkumar, M., Ravichandran, M., 2012. The influences of ENSO on tropical cyclone activity in the Bay of Bengal during October–December. J. Geophys. Res.: Oceans 117.
Gori, A., Lin, N., Xi, D., Emanuel, K., 2022. Tropical cyclone climatology change greatly exacerbates US extreme rainfall–surge hazard. Nat. Clim. Change 12, 171–178.
Greiving, S., 2006. Integrated risk assessment of multi-hazards: a new methodology. Spec. Pap. Geol. Surv. Finland 42, 75.
Haque, A., Nicholls, R.J., 2018. Floods and the Ganges-Brahmaputra-Meghna Delta. Ecosystem Services for Well-Being in Deltas: Integrated Assessment for Policy Analysis, pp. 147–159.
Hoque, M.A.-A., Phinn, S., Roelfsema, C., Childs, I., 2016. Assessing tropical cyclone impacts using object-based moderate spatial resolution image analysis: a case study in Bangladesh. Int. J. Rem. Sens. 37, 5320–5343.
Hoque, M.A.-A., Phinn, S., Roelfsema, C., Childs, I., 2017. Tropical cyclone disaster management using remote sensing and spatial analysis: a review. Int. J. Disaster Risk Reduc. 22, 345–354.
Hoque, M.A.-A., Pradhan, B., Ahmed, N., Ahmed, B., Alamri, A.M., 2021. Cyclone vulnerability assessment of the western coast of Bangladesh. Geomatics, Nat. Hazards Risk 12, 198–221.
Hoque, M.A.-A., Pradhan, B., Ahmed, N., Roy, S., 2019. Tropical cyclone risk assessment using geospatial techniques for the eastern coastal region of Bangladesh. Sci. Total Environ. 692, 10–22.
Islam, M.A., Mitra, D., Dewan, A., Akhter, S.H., 2016. Coastal multi-hazard vulnerability assessment along the Ganges deltaic coast of Bangladesh–A geospatial approach. Ocean Coast Manag. 127, 1–15.
Islam, S.N., Reinstädtler, S., Ferdaush, J., 2017. Challenges of climate change impacts on urban water quality management and planning in coastal towns of Bangladesh. Int. J. Environ. Sustain Dev. 16, 228–256.
Jenks, G.F., 1967. The data model concept in statistical mapping. Int. Yearb. Cartogr. 7, 186–190.
Juarez Garcia, H., 2010. Multi-hazard Risk Assessment: an Interdependency Approach. University of British Columbia.
Kappes, M.S., Keiler, M., von Elverfeldt, K., Glade, T., 2012. Challenges of analyzing multi-hazard risk: a review. Nat. Hazards 64, 1925–1958.
Karra, K., Kontgis, C., Statman-Weil, Z., Mazzariello, J.C., Mathis, M., Brumby, S.P., 2021. Global Land Use/land Cover with Sentinel 2 and Deep Learning, 2021 IEEE International Geoscience and Remote Sensing Symposium IGARSS. IEEE, pp. 4704–4707.
Kubler, S., Robert, J., Derigent, W., Voisin, A., Le Traon, Y., 2016. A state-of the-art survey & testbed of fuzzy AHP (FAHP) applications. Expert Syst. Appl. 65, 398–422.
Kumar, S., Lal, P., Kumar, A., 2020. Turbulence of tropical cyclone 'fani'in the Bay of bengal and Indian subcontinent. Nat. Hazards 103, 1613–1622.
Liu, B., Siu, Y.L., Mitchell, G., 2016. Hazard interaction analysis for multi-hazard risk assessment: a systematic classification based on hazard-forming environment. Nat. Hazards Earth Syst. Sci. 16, 629–642.
Miah, M.Y., Kamal, M.Z.U., Salam, M.A., Islam, M.S., 2020. Impact of salinity intrusion on agriculture of Southwest Bangladesh-A review. Int. J. Agric. Pol. Res.
Ming, X., Liang, Q., Dawson, R., Xia, X., Hou, J., 2022. A quantitative multi-hazard risk assessment framework for compound flooding considering hazard inter-dependencies and interactions. J. Hydrol. 607, 127477.
Montibeller, G., Franco, A., 2010. Multi-criteria Decision Analysis for Strategic Decision Making, Handbook of Multicriteria Analysis. Springer, pp. 25–48.
Murty, T., Flather, R., 1994. Impact of storm surges in the Bay of bengal. J. Coast Res. 149–161.
Naghadehi, M.Z., Jimenez, R., KhaloKakaie, R., Jalali, S.-M.E., 2011. A probabilistic systems methodology to analyze the importance of factors affecting the stability of rock slopes. Eng. Geol. 118, 82–92.
Pearl, J., 2011. Bayesian Networks.
Pouyakian, M., Khatabakhsh, A., Yazdi, M., Zarei, E., 2022. Optimizing the allocation of risk control measures using fuzzy MCDM approach: review and application. In: Linguistic Methods under Fuzzy Information in System Safety and Reliability Analysis, pp. 53–89.
Raja, D.R., Hredoy, M.S.N., Islam, M.K., Islam, K.A., Adnan, M.S.G., 2021. Spatial distribution of heatwave vulnerability in a coastal city of Bangladesh. Environmental Challenges 4, 100122.
Sahoo, B., Bhaskaran, P.K., 2018. Multi-hazard risk assessment of coastal vulnerability from tropical cyclones–A GIS based approach for the Odisha coast. J. Environ. Manag. 206, 1166–1178.
Salman, M.A., 2023. Assessment of vulnerability and capacity to the cyclone 'Amphan'impacts of the southwestern coastal part of Bangladesh: an empirical contextual investigation. Nat. Hazards 115, 1715–1742.
Sarwar, G.M., 2008. Landslide Tragedy of Bangladesh. The first world landslide forum.
Shaw, R., Mallick, F., Islam, A., 2013. Climate Change Adaptation Actions in Bangladesh. Springer.
Siam, Z.S., Hasan, R.T., Anik, S.S., Noor, F., Adnan, M.S.G., Rahman, R.M., Dewan, A., 2022. National-scale flood risk assessment using GIS and remote sensing-based hybridized deep neural network and fuzzy analytic hierarchy process models: a case of Bangladesh. Geocarto Int. 37, 12119–12148.
Steele, J.E., Sundsøy, P.R., Pezzulo, C., Alegana, V.A., Bird, T.J., Blumenstock, J., Bjelland, J., Engø-Monsen, K., De Montjoye, Y.-A., Iqbal, A.M., 2017. Mapping poverty using mobile phone and satellite data. J. R. Soc. Interface 14, 20160690.
Talchabhadel, R., Maskey, S., Gouli, M.R., Dahal, K., Thapa, A., Sharma, S., Dixit, A.M., Kumar, S., 2023. Multimodal multiscale characterization of cascading hazard on mountain terrain. Geomatics, Nat. Hazards Risk 14, 2162443.
Tilloy, A., Malamud, B.D., Winter, H., Joly-Laugel, A., 2019. A review of quantification methodologies for multi-hazard interrelationships. Earth Sci. Rev. 196, 102881.
Tiwari, G., Rameshan, A., Kumar, P., Javed, A., Mishra, A.K., 2022. Understanding the post-monsoon tropical cyclone variability and trend over the Bay of Bengal during the satellite era. Q. J. R. Meteorol. Soc. 148, 1–14.
Wachinger, G., Renn, O., Begg, C., Kuhlicke, C., 2013. The risk perception paradox—implications for governance and communication of natural hazards. Risk Anal. 33, 1049–1065.
Ward, P.J., Blauhut, V., Bloemendaal, N., Daniell, J.E., de Ruiter, M.C., Duncan, M.J., Emberson, R., Jenkins, S.F., Kirschbaum, D., Kunz, M., 2020. Natural hazard risk assessments at the global scale. Nat. Hazards Earth Syst. Sci. 20, 1069–1096.
Yang, X.-l., Ding, J.-h., Hou, H., 2013. Application of a triangular fuzzy AHP approach for flood risk evaluation and response measures analysis. Nat. Hazards 68, 657–674.